Anatomy of Sigma of a Global Intensity-Measure Prediction Model

Schweizerischer Erdbebendienst
Service Sismologique Suisse
Servizio Sismico Svizzero
Swiss Seismological Service

ETH
Eidgenössische Technische Hochschule Zürich
Swiss Federal Institute of Technology Zurich

Carlo Cauzzi(1) & Ezio Faccioli(2)

(1) Swiss Seismological Service at ETH Zürich

(2) Politecnico di Milano & Studio Geotecnico Italiano

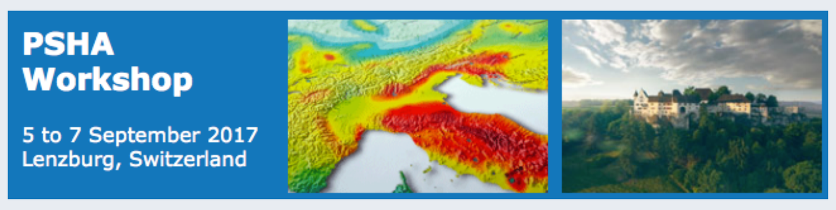

We present a scrutiny of the components of uncertainty of our recent predictive model (Cauzzi et al., 2015), with emphasis on their possible dependence on basic model predictors and source region. We follow the standard nomenclature of Strasser et al. (2009) and Al Atik et al. (2010). Our dataset does not support the adoption of a magnitude-dependent ϕ or τ model, although there is evidence to suggest that τ of large-magnitude events is lower than that of moderate- and small-magnitude events for vibration periods T < ~ 3 s. The distance dependence of ϕ and ϕ_{SS} in our data is unclear, but near-source residuals exhibit comparatively larger variability, especially at intermediate and long periods, most likely due to the absence of near-source terms (e.g., hanging-wall, directivity) in our predictive model. The variability of the δWes residuals segregated by ground type is inflated at the dominant amplification periods of the site response, and the residuals on EC8 ground-type A are associated with the lowermost spread. The regional dependence of the δWes residuals in our dataset is small up to intermediate periods, and the offset of regional sub-populations with respect to the overall mean of the residuals is practically equal to zero. ϕ_{S2S} and ϕ_{SS} computed based on stations with at least 4 records are in good agreement with previously published global and regional models, confirming the limited dependence of ϕ_{SS} on source region and ground type. Compared to other studies, our τ model is enlarged by Pan-European events terms associated to reverse faults. The contribution to τ of poorly recorded events (with less than three records) is effectively minimised by the weighting scheme of Joyner and Boore (1993 and 1994) that we used to develop our predictive equations.

(1) Within-event uncertainty component ϕ = st.dev.(δW_{es})

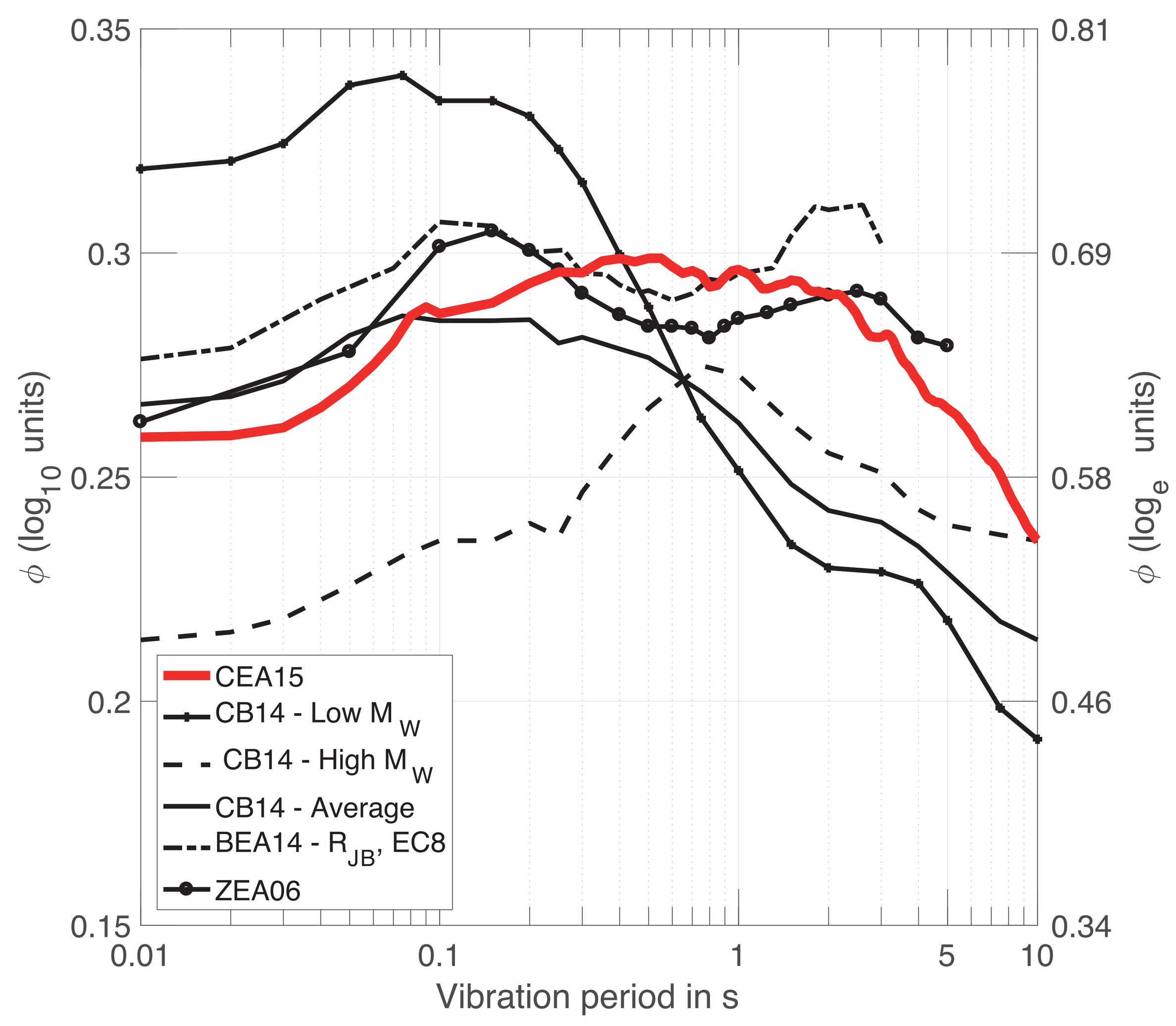

Within-event uncertainty component, ϕ, of Cauzzi et al. (2015) - CEA15 - compared to that of other global (Campbell and Bozorgnia, 2014 - CB14) and regional (Bindi et al., 2014 - BEA14; Zhao et al., 2006 - ZEA06) studies. Note that ϕ of CB14 is modelled as heteroscedastic with respect to Mw.

Ground-motion prediction model:

$$y = f_M(M_W, M_W^2, \text{style of faulting}) +$$
$$+ f_R(R_{RUP}, M_W) +$$
$$+ f_S(EC8, V_{S,30})$$

Two-step maximum-likelihood regressions (Joyner and Boore, 1993 and 1994):

(1st step): f_R, f_S, ϕ
(2nd step): f_M, τ

Data from different regions with active shallow crustal seismicity. Mainly Japan due to high-quality digital data and metadata. Other data included to fill gaps in M_W-R_{RUP} distribution.

Regional dependence originally (Cauzzi and Faccioli, 2008) excluded based on ANOVA.

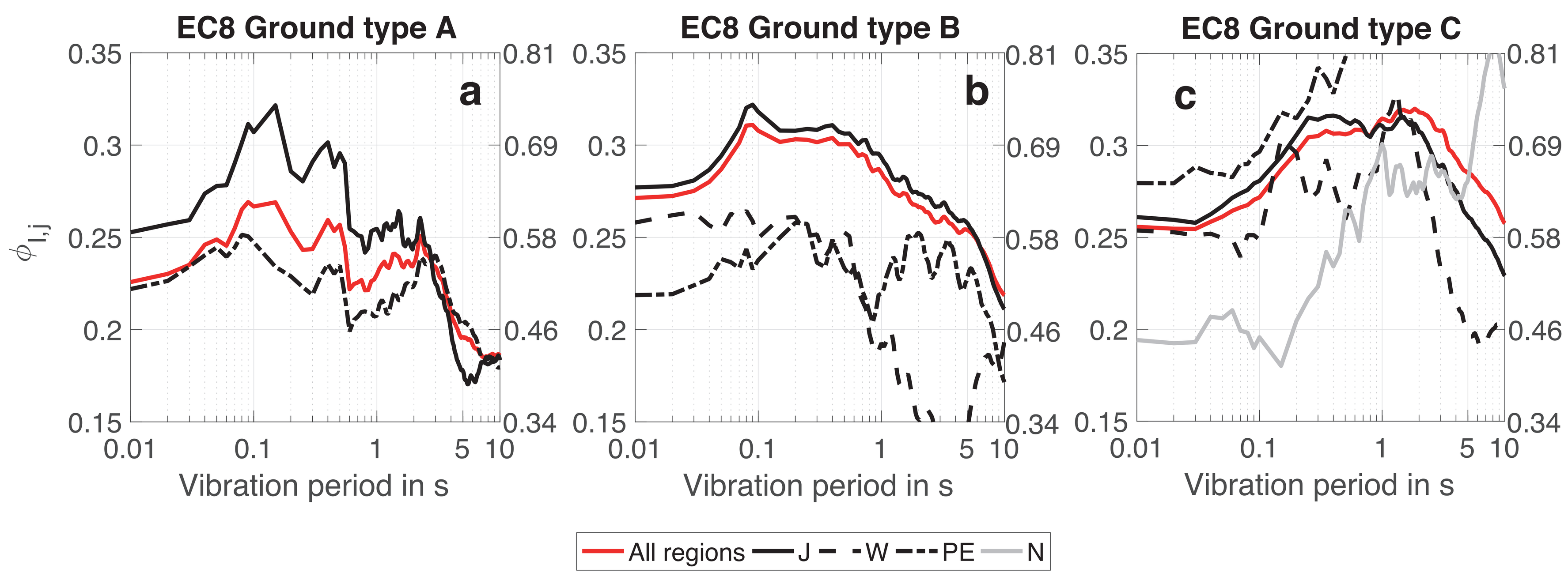

Regional (Japan, Western USA, Pan-Europe, New Zealand) and ground-type components of ϕ of CEA15 based on subpopulations of δW_{es} with at least 30 data. Data from New Zealand are actually representative of the Canterbury Plains only.

(2) Between-events uncertainty component τ = st.dev.(δB_e^B)

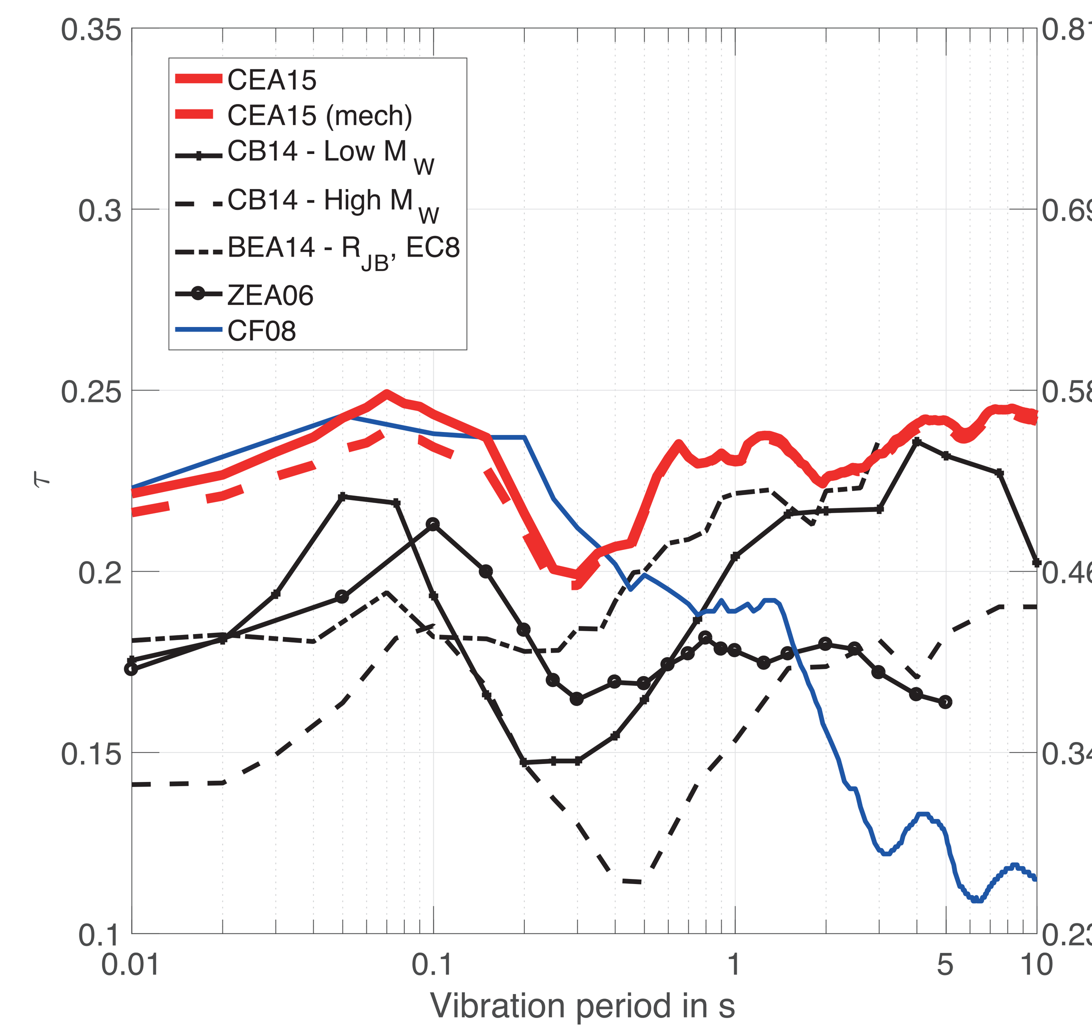

Between-events uncertainty component, τ, of Cauzzi et al. (2015) - CEA15 - compared to that of other global (Campbell and Bozorgnia, 2014 - CB14) and regional (Bindi et al., 2014 - BEA14; Zhao et al., 2006 - ZEA06) studies. Note that τ of CB14 is modelled as heteroscedastic with respect to Mw.

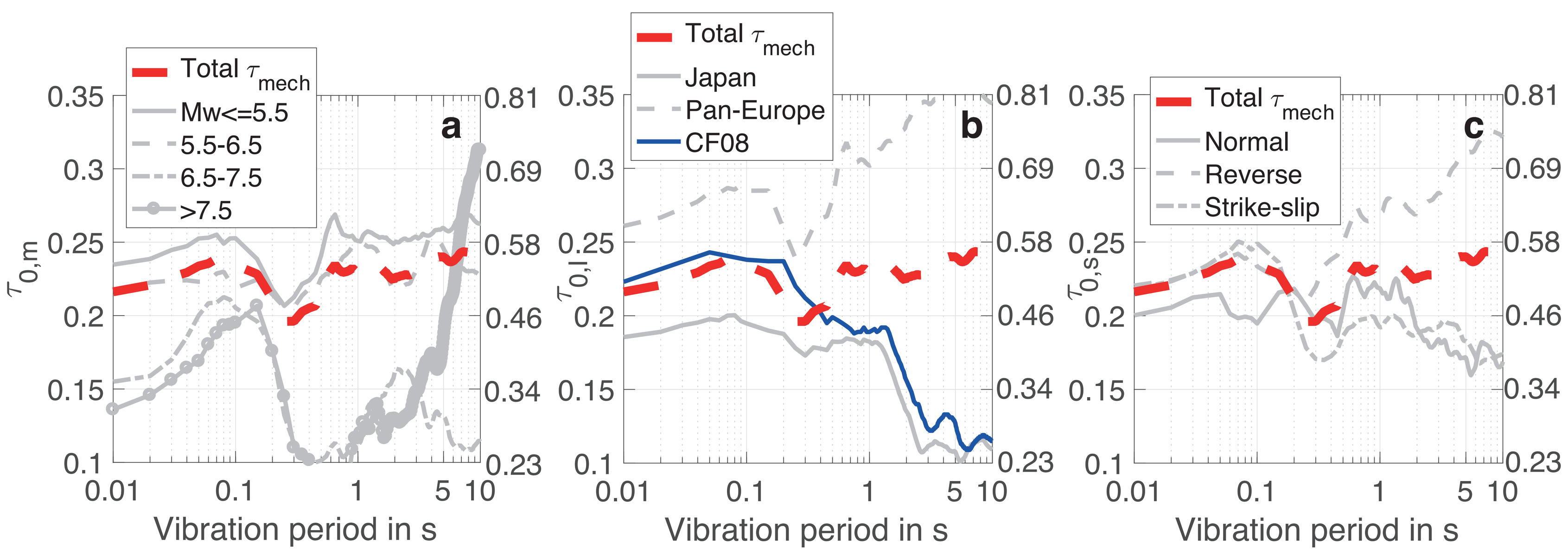

Total τ_{mech} of CEA15 and its dependence on moment magnitude (a), region (b), and faulting style (c) The grey curves in the picture are computed from subsets of the CEA15 δB_e^B population. The blue curve in panel (b) is the τ_{mech} model of Cauzzi and Faccioli (2008) - CF08.

(1.1) Single-site ϕ_{SS} = st.dev (δWS_{es})

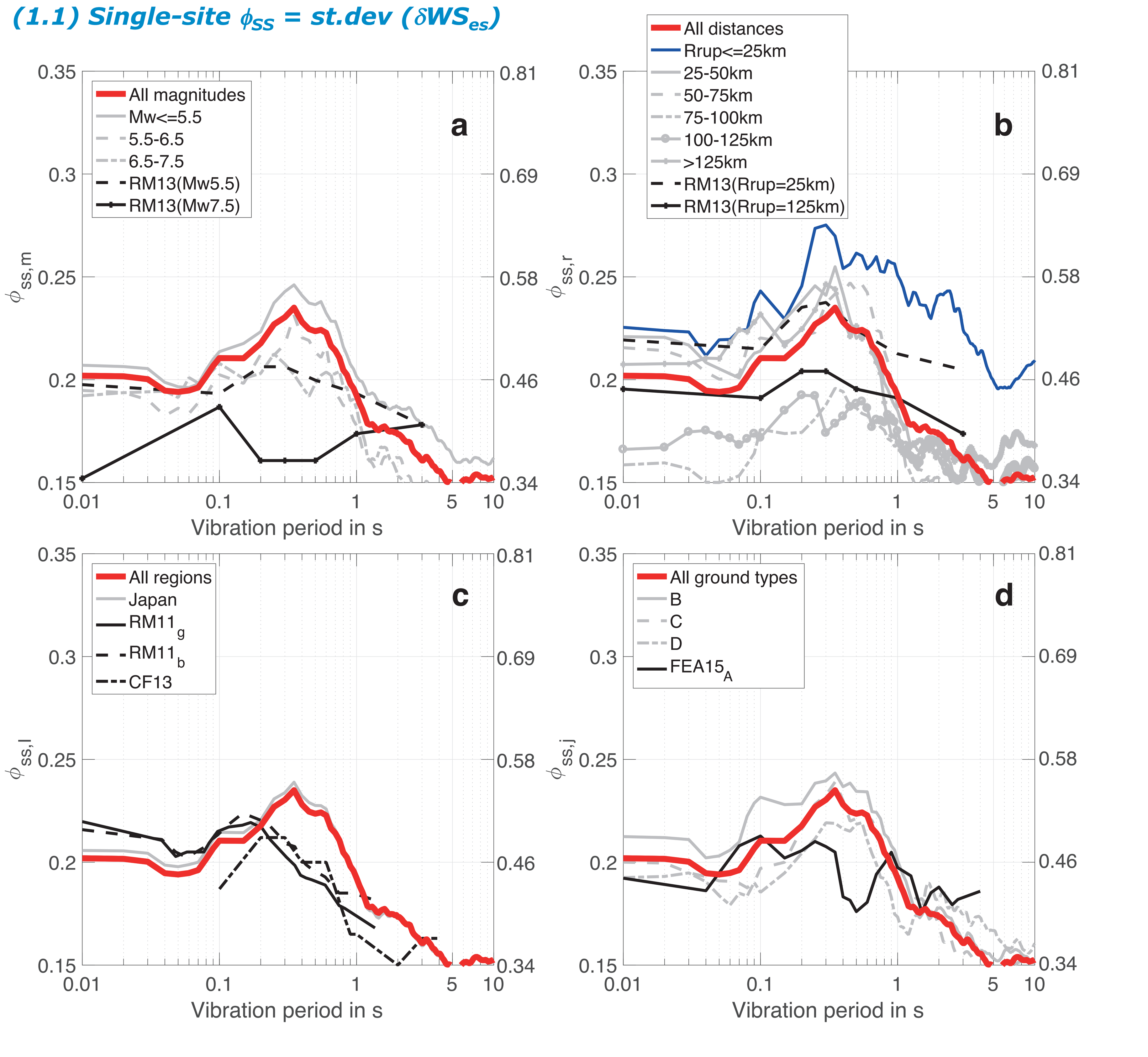

Total ϕ_{SS} of CEA15 (the red curves) computed based on stations with at least four records, and its dependence on moment magnitude (a), rupture distance (b), region (c), and EC8 ground type (d). The grey and blue curves in the picture are computed based on subsets of the CEA15 δWS_{es} population. The black curves shown for comparison are the surface and borehole models Rodriguez-Marek et al. (2011) - RM11g and RM11b, the global model Rodriguez-Marek et al. (2013) - RM13, the New Zealand (Canterbury region) model Chen and Faccioli (2013) - CF13, and the Italian rock model of Faccioli et al. (2015) - FEA15.

(2.1) Focus on region and SOF dependence of τ

Total τ_{mech} of CEA15 compared with the weighted standard deviation $\tau_{0,s,l}$ of the between-events residuals sorted by region (Japan and Pan-Europe) and style-of-faulting. Out of nine reverse-fault events, only two Iranian earthquakes were already included in the CF08 dataset. The remaining seven all pertain to the 2012 Emilia (Northern Italy) seismic sequence, that is apparently playing a significant role in inflating τ_{mech} of CEA15 at intermediate and long periods. It is likely that peculiarities in the site response like, e.g., complex basin effects in the Po alluvium plain not modelled in the first stage of the regressions, are propagated to the subsequent stages and are inflating τ_{mech}. The blue curve is obtained neglecting the event terms of the Emilia sequence. It is proposed as alternative τ model for CEA15.

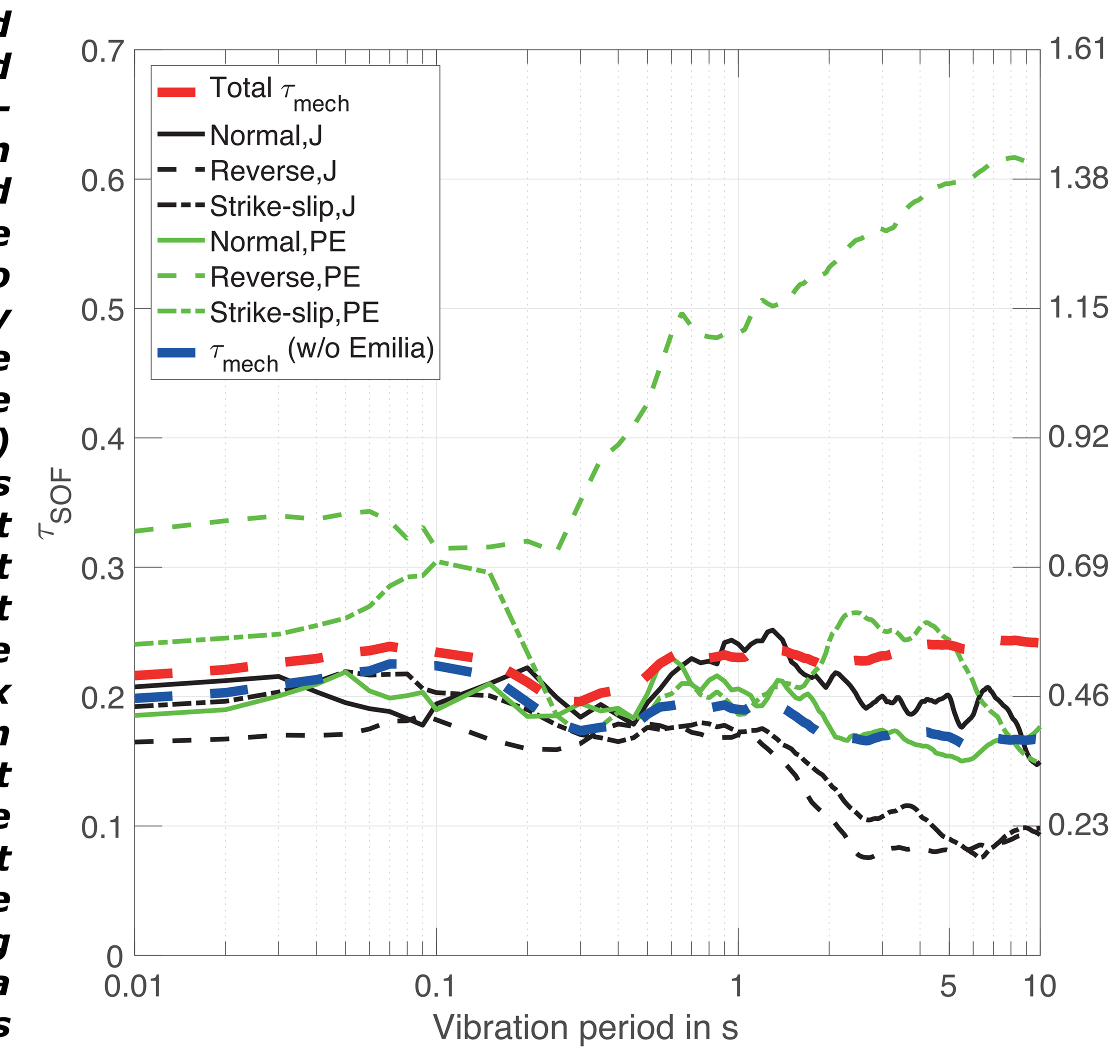

Key References

- Al Atik L, Abrahamson N, Bommer JJ, et al (2010) The Variability of Ground-Motion Prediction Models and Its Components. Seismol Res Lett 81:659–801. doi: 10.1785/gssrl.81.5.794
- Bindi D, Massa M, Luzi L, et al (2013) Pan-European ground-motion prediction equations for the average horizontal component of PGA, PGV, and 5 %-damped PSA at spectral periods up to 3.0 s using the RESORCE dataset. Bull Earthq Eng 12:391–430. doi: 10.1007/s10518-013-9525-5
- Campbell KW, Bozorgnia Y (2014) NGA-West2 Ground Motion Model for the Average Horizontal Components of PGA, PGV, and 5% Damped Linear Acceleration Response Spectra. Earthq Spectra 30:1087–1115. doi: 10.1193/062913EQS175M
- Cauzzi C, Faccioli E, Vanini M, Bianchini A (2015) Updated predictive equations for broadband (0.01–10 s) horizontal response spectra and peak ground motions, based on a global dataset of digital acceleration records. Bull Earthq Eng 13:1587–1612. doi: 10.1007/s10518-014-9685-y
- Cauzzi C, Faccioli E (2008) Broadband (0.05 to 20 s) prediction of displacement response spectra based on worldwide digital records. J Seismol 12:453–475. doi: 10.1007/s10950-008-9098-y
- Chen L, Faccioli E (2013) Single-station standard deviation analysis of 2010--2012 strong-motion data from the Canterbury region, New Zealand. Bull Earthq Eng 11:1617–1632. doi: 10.1007/s10518-013-9454-3
- Faccioli E, Paolucci R, Vanini M (2015) Evaluation of Probabilistic Site-Specific Seismic-Hazard Methods and Associated Uncertainties, with Applications in the Po Plain, Northern Italy. Bull Seismol Soc Am . doi: 10.1785/0120150051
- Joyner WB, Boore DM (1994) Methods for regression analysis of strong-motion data. Bull Seismol Soc Am 84:955–956.
- Joyner WB, Boore DM (1993) Methods for regression analysis of strong-motion data. Bull Seismol Soc Am 83:469–487.
- Rodriguez-Marek A, Montalva GA, Cotton F, Bonilla F (2011) Analysis of Single-Station Standard Deviation Using the KiK-net Data. Bull Seismol Soc Am 101:1242–1258. doi: 10.1785/0120100252
- Rodriguez-Marek A, Cotton F, Abrahamson NA, et al (2013) A Model for Single-Station Standard Deviation Using Data from Various Tectonic Regions. Bull Seismol Soc Am 103:3149–3163. doi: 10.1785/0120130030
- Strasser FO, Abrahamson NA, Bommer JJ (2009) Sigma: Issues, Insights, and Challenges. Seismol Res Lett 80:40 LP-56.
- Zhao JX, Zhang J, Asano A, et al (2006) Attenuation Relations of Strong Ground Motion in Japan Using Site Classification Based on Predominant Period. Bull Seismol Soc Am 96:898–913. doi: 10.1785/0120050122